HHS Public Access

Author manuscript

Science. Author manuscript; available in PMC 2019 July 24.

Published in final edited form as:

Science. 2018 November 09; 362(6415): 694–699. doi:10.1126/science.aat5030.

WDFY4 is required for cross-presentation in response to viral and tumor antigens

Derek J. Theisen[1,†], **Jesse T. Davidson IV**[1,2,†], **Carlos G. Briseño**[1], **Marco Gargaro**[3], **Elvin J. Lauron**[4], **Qiuling Wang**[5], **Pritesh Desai**[1,5], **Vivek Durai**[1], **Prachi Bagadia**[1], **Joshua R. Brickner**[1], **Wandy L. Beatty**[5], **Herbert W. Virgin**[1,6], **William E. Gillanders**[2,7], **Nima Mosammaparast**[1], **Michael S. Diamond**[1,5,8,9], **L. David Sibley**[5], **Wayne Yokoyama**[4], **Robert D. Schreiber**[1,9], **Theresa L. Murphy**[1], **Kenneth M. Murphy**[1,10,*]

[1]Department of Pathology and Immunology, Washington University in St. Louis, School of Medicine, St. Louis, MO 63110, USA

[2]Department of Surgery, Washington University in St. Louis, School of Medicine, St. Louis, MO 63110, USA

[3]Department of Experimental Medicine, University of Perugia, Perugia, Italy

[4]Division of Rheumatology, Department of Medicine, Washington University in St. Louis, School of Medicine, St. Louis, MO 63110, USA

[5]Department of Molecular Microbiology, Washington University in St. Louis, School of Medicine, St. Louis, MO 63110, USA

[6]Vir Biotechnology, San Francisco, CA, USA

[7]The Alvin J. Siteman Cancer Center at Barnes-Jewish Hospital and Washington University School of Medicine, St. Louis, MO 63110, USA

[8]Department of Medicine, Washington University School of Medicine, St. Louis, MO 63110, USA

[9]Andrew M. and Jane M. Bursky Center for Human Immunology and Immunotherapy Programs, Washington University School of Medicine, St. Louis, MO 63110, USA

[10]Howard Hughes Medical Institute, Washington University in St. Louis, School of Medicine, St. Louis, MO 63110, USA

Abstract

[*]To whom correspondence should be addressed. Phone: 314-362-2009, kmurphy@wustl.edu.

[†]These authors contributed equally to this work

Author contributions: D.J.T. and J.T.D. contributed equally to this work and designed, performed, and analyzed most experiments. C.G.B. and P.B. performed and analyzed experiments. V.D., M.G., E.J.L., W.Y., Q.W., L.D.S., W.L.B., J.R.B., N.M., P.D., and M.S.D. designed, performed, and analyzed experiments. R.D.S generated models and designed experiments. W.E.G., T.L.M., K.M.M., designed experiments and wrote manuscript.

Competing interests: H.W.V. is a founder of Casma Therapeutics, Cambridge, MA.

Data and materials availability: Microarray data has been deposited in the NCBI gene expression omnibus at accession number GSE118652, Proteomics data has been deposited in the Proteomics Identifications (PRIDE) archive px-submission #298619 (accession # PENDING), all other data is available in manuscript or supplementary materials. WDFY4 knockout mice were generated by and are available through the KOMP[2] program at The Jackson Laboratory (029334).

During the process of cross presentation, viral or tumor-derived antigens are presented to $CD8^+$ T cells by the *Batf3*-dependent $CD8\alpha^+/XCR1^+$ classical dendritic cell (cDC1). We designed a functional CRISPR screen for novel regulators of cross presentation, and identified the BEACH-domain containing protein WDFY4 as essential for cross-presentation of cell-associated antigens by cDC1. WDFY4 was not, however, required for MHC class II presentation or for cross-presentation by monocyte-derived DCs. In contrast to *Batf3*$^{-/-}$ mice, *Wdfy4*$^{-/-}$ mice have normal lymphoid and non-lymphoid cDC1 populations that produce IL-12 and protect against *Toxoplasma gondii* infection. However similar to *Batf3*$^{-/-}$ mice, *Wdfy4*$^{-/-}$ mice fail to prime virus- specific $CD8^+$ T cells *in vivo* or induce tumor rejection, revealing a critical role for cross-presentation in anti-viral and anti-tumor immunity.

One Sentence Summary:

WDFY4 is required for cross-presentation *in vivo,* and is necessary for anti-viral and anti-tumor immunity.

Presentation of antigens as peptides bound to proteins of the major histocompatibility complex (MHC) is the principal mechanism by which innate cells promote antigen-specific T cell immunity (1). Classical dendritic cells (cDC) are particularly efficient antigen presenting cells and comprise two major functionally distinct subsets, the cDC1 and cDC2 (2–4). The cDC1 lineage (2,5) is the most efficient at priming cytotoxic $CD8^+$ T cells to exogenously-derived antigens, a process termed cross-presentation (6–10). This specialization was observed in *Batf3*$^{-/-}$ mice that specifically lack cDC1 development and cannot mount cytotoxic T cell responses to viruses and tumors (10–24). However, since these studies have only analyzed these responses in the context of mice lacking cDC1, the role of cross-presentation versus other cDC1-specific effector functions, such as IL-12 mediated protection against *Toxoplasma gondii* (25), has remained incompletely understood.

Cross-presentation has been studied using different cell types and various forms of antigen, and not all findings have been confirmed *in vivo* (26). DCs generated from monocytes (moDCs) or whole bone marrow cultured *in vitro* with GM-CSF with or without IL-4 (27–29) are heterogeneous, resembling both macrophages and DCs (30), and use a cross-presentation program divergent from the cDC1 *in vivo* (26,31,32). Studies of moDCs have produced two major models of cross-presentation; one that involves transport of exogenous antigen to the cytosolic proteasome before peptide loading in the endoplasmic reticulum (ER) (1,7,33–35), and another where peptide loading occurs directly in phagosomes by fusion with vesicles containing the peptide-loading-complex (36,37). The latter pathway may be regulated by the SNARE family member Sec22b, although two recent studies of *Sec22b* deficient mice arrived at different conclusions as to the role of Sec22b in T cell priming to cell-associated antigens *in vivo* (38,39). These differences highlight the need for systematic investigation into the mechanisms of cross-presentation *in vivo* (39,40).

We established a screen for novel cellular components required for cross-presentation, and optimized *in vitro* conditions to replicate this process in cDC1. The efficiency and cell-type specificity of cross-presentation can vary, depending on whether the antigen is soluble or associated with cells or pathogens (32). Bacterial-associated antigen in the form of heat-

killed *Listeria monocytogenes* expressing ovalbumin (HKLM-OVA) is efficiently cross-presented by cDC1 to OT-I T cells, but not presented by cDC2 (Fig. 1A). In contrast, soluble OVA is crosspresented by both cDC1 and cDC2 lineages, with 3–10 fold lower efficiency in cDC2 (Fig. 1B). Presentation of SIINFEKL peptide to OT-I cells is equally efficient in cDC1 and cDC2, as expected (Fig. 1C). Previous studies have suggested that the majority of antigens undergo translocation to the cytosol during cross-presentation *in vivo* (1,7,35). We found that cell-associated antigens, which are presented only by cDC1 and not cDC2, are *Tap1*-dependent, suggesting presentation through the cytosolic pathway (Fig. 1D). In contrast, soluble antigens were presented by both *Tap1*$^{-/-}$ cDC1 and cDC2, with only slight differences in efficiency compared to WT cDCs (Fig. 1E). For these reasons, we concluded that use of cell-associated antigens in a screen would best emphasize cDC1-specific processing functions.

Screening could be done using either biochemical detection of peptide:MHC complexes (p:MHC) or using a T cell response. The antibody 25-D1.16 can directly measure SIINFEKL:K^{b} complexes on the cell surface (41). 25-D1.16 detected a robust signal from soluble OVA processed by cDC1 (Fig. 1F), but no signal was detected using an immunogenic dose of cell-associated antigen (Fig. 1G). T cells can respond to only a few hundred p:MHC (42,43), implying that the detection limit for 25-D1.16 is greater than that for T cells. Thus, we decided to use T cell proliferation as the readout and determined that 10^4 cDCs can produce reliable and specific signal of OT-I proliferation (Fig. 1H). We considered gene candidates based on expression in cDCs, relative cDC1 specificity and gene ontology (Table S1). We expressed single guide RNAs (sgRNAs) (44) for candidates (Table S2) by retrovirus under the U6 promoter and infected DC progenitors from Cas9 transgenic mice (45) (fig. S1A). Cells were cultured in Flt3L for 7d, sorted to purify infected cDCs, and tested for cross-presentation (Fig. 1I, fig. S1B,C).

Cross-presentation was substantially impaired by two independent sgRNAs for WD Repeat- and FYVE Domain-Containing Protein 4 (*Wdfy4*), a member of the BEACH (Beige and Chediak-Higashi) domain containing family of proteins (46) (Fig. 2A, fig S1C). WDFY4 is highly expressed in mouse and human cDC1 (fig S2), with 80% species similarity (47). Wdfy4 is one of 9 BEACH-domain containing proteins (46) and has three closely related family members. However, CRISPR targeting using sgRNAs for *Wdfy1, Wdfy2, Wdfy3* did not impair cross-presentation, in contrast to *Wdfy4* (Fig. 2B). Thus, *Wdfy4* appears to be unique within this gene family for supporting cross-presentation by cDC1.

To evaluate the *in vivo* function of *Wdfy4,* we obtained mice with exon 4 deleted by CRISPR/Cas9 genome editing, leading to translational termination due to a reading frame shift when exon 3 splices to exon 5 (fig. S3). *Wdfy4*$^{-/-}$ mice are viable, born in normal Mendelian ratios and have normal development of hematopoietic lineages, including cDCs (Fig. 2C and D, fig. S4), which express *Irf8* and have normal turnover kinetics (fig. S4H and I), and T cells (fig. S5). In particular, cDC1 develop in *Wdfy4*$^{-/-}$ mice, unlike *Batf3*$^{-/-}$ mice, and express CD24, XCR1 and CD103 normally (Fig. 2 C and D, fig. S4B and F). However, cDC1 from *Wdfy4*$^{-/-}$ mice show a striking defect in cross-presentation of both cell-associated and bacterial-associated antigen *in vitro* (Fig. 2 E and F, fig. S6A) and show reduced efficiency for soluble OVA presentation compared with WT cDC1 (Fig. 2G).

Notably, *Wdfy4*$^{-/-}$ cDC1 cross-present soluble OVA with the efficiency of cDC2, which are not influenced by the loss of *Wdfy4* (Fig. 2G). However, *Wdfy4*$^{-/-}$ cDC1 can directly present antigen introduced into the cytoplasm by osmotic shock or virus, a process that is equally efficient in cDC1 and cDC2 (fig. S6B to D), suggesting that *Wdfy4*$^{-/-}$ cDC1 have the capacity to present endogenous antigens on MHCI.

MoDCs can cross-present both soluble and cell-associated antigens *in vitro* (27,48,49), but use a distinct transcriptional program from cDC1 (31). We find that moDCs derived from WT and *Wdfy4*$^{-/-}$ mice cross-present antigens with the same efficiency, both for cell-associated (fig. S6E) and soluble OVA (fig. S6F), suggesting that moDCs use a *Wdfy4-independent* pathway for cross-presentation. The defect in cross-presentation by *Wdfy4*$^{-/-}$ cDC1 is specific, since MHC class II antigen processing was unchanged in *Wdfy4*$^{-/-}$ mice for both cell-associated and soluble antigens (Fig. 2H; fig. S6G). MHC class II antigen processing by B cells is also normal in *Wdfy4*$^{-/-}$ mice (fig. S7A), which are able to generate germinal center B cells and T follicular helper (T_{FH}) cells in response to immunization with sheep red blood cells (fig. S7B to E).

cDCs from *Wdfy4*$^{-/-}$ mice expressed normal levels of MHCI at steady state and after activation (fig. S8A and B), upregulated costimulatory molecules CD80/86 and expressed cytokines normally (fig S8C to F). Loss of *Wdfy4* also did not influence gene expression in cDC1s at steady state or after activation in tumor-bearing mice (fig. S8G and H). Despite their inability to cross-present, *Wdfy4*$^{-/-}$ cDC1 are capable of taking up and degrading soluble antigens normally (fig. S9A and B) and phagocytosing labeled HKLM-OVA, as seen both microscopically (fig. S9C) and by quantification of this phagocytosis as measured by FACS (fig. S9D).

To explore the mechanism of action of WDFY4, we analyzed various cellular compartments of wild-type and *Wdfy4*$^{-/-}$ cDC1 by confocal microscopy and found minimal differences in distribution of MHCI stores, ER, early endosomes, lysosomes, late endosomes, or the peptide-loading complex at steady state (fig. S10) or Rab43 (a molecule previously described to be involved in cross-presentation (32)), p62 (autophagic vesicles), Rab7 (late endosomes), or Lamp1 (lysosomes) after antigen phagocytosis (fig. S11). Electron microscopy of WDFY4-deficient *ex vivo* cDC1 showed the presence of large and numerous lipid bodies throughout the cytoplasm that were not present in wild-type cells (fig. S12, fig. S13A and C). However, these lipid bodies were not present in Flt3L-derived cDC1 from *Wdfy4*$^{-/-}$ mice (S13B and C), which still have a defect in cross-presentation of cell-associated antigen (fig. S13D), suggesting that the lipid bodies are not necessary to cause the defect in cross-presentation in *Wdfy4*$^{-/-}$ cDC1.

To determine interacting partners of WDFY4, we generated four individually FLAG-tagged sub-regions of WDFY4 spanning the entire protein (Fig. 3A). We stably transduced these fragments into the murine DC line JAWSII (50), and performed affinity purification-mass spectrometry (AP-MS) to isolate WDFY4 binding partners. We found 143 candidates enriched by different regions of the WDFY4 protein, with the largest number binding to the FL4 fragment of WDFY4 that contains the PH, BEACH, WD40, and FYVE domains (Fig. 3A, Table S3). We performed gene ontology analysis to determine the biological processes

most likely influenced by WDFY4 (51). The fragments FL1 and FL2 of WDFY4 associated with proteins involved in “protein complex assembly,” and therefore may be involved in forming multimeric protein structures or scaffolding vesicular machinery (Fig. 3B, Table S4). FL3 and FL4 associated with proteins involved in “protein localization,” “vesicle transport,” and “cytoskeletal organization,” suggesting a role for WDFY4 in proper subcellular vesicular targeting (Fig. 3C, Table S5). Notably, FL4 associated with components critical to the formation, function, and trafficking of endocytic vesicles, including clathrin (*Cltc, Clta*) (52), subunits of the AP-2 clathrin adaptor complex (*Ap2a1, Ap2a2, Ap2b1*) (52), modulators of cytoskeleton dynamics (*Iqgap1, Actn4*) (53,54), and several members of the vacuolar-type (H^+) ATPase (*Atp6v0a3, Atp6va1, Atp6v1f*) (55) (Fig. 3D, Table S3 and S6). FL4 also selectively associated with *Hsp90ab1,* a member of the HSP90 chaperone family involved in endosome-to-cytosol translocation of antigen during cross-presentation (56–59) (Figure 3D to F). While heat-shock proteins such as *Hspa8* and *Hsp1a1* can appear as artefacts in AP-MS data due to their function as chaperones (60), *Hsp90ab1* is rarely detected in this manner, and therefore its association may represent a functional interaction with WDFY4.

We then sought to determine which vesicles WDFY4 may be acting on by determining its intracellular location. We visualized full-length Twin-Strep-tagged (61) WDFY4 in JAWSII cells by confocal microscopy and found that it localized to the periphery of the cytosol near the plasma membrane (Fig 3G). WDFY4 was poorly co-localized with the cell surface receptor DEC-205, intracellular MHCI stores and lysosomes, but demonstrated moderate co-localization with early endosomes and the ER. cDC1 have been previously shown to have well defined and extensive ER structures which may extend throughout the cytosol near vesicular compartments (62), and lead to co-localization with components of the endosomal pathway. WDFY4 shows highest correlation with endosomal markers clathrin and Rab11 (Fig 3G and H), suggesting that it localizes to an endosomal compartment near the plasma membrane. Taken together, these data suggest that WDFY4 functions in trafficking between the cell surface and endosomes and thus may regulate multimeric protein assembly required for proper formation and localization of endocytic vesicles.

We then examined the role of WDFY4 in cross-presentation of cell-associated antigens *in vivo.* CFSE-labeled OT-I T cells showed strong *in vivo* proliferation induced by immunization with OVA-loaded splenocytes when transferred into *Wdfy4*$^{+/-}$ mice, but not *Wdfy4*$^{-/-}$ mice (Fig. 4A and B), confirming an *in vivo* defect in cross-presentation. IL-12 produced by cDC1 in response to soluble tachyzoite antigen (STAg) is required for innate immune protection against *T. gondii,* as illustrated by the susceptibility of *Batf3*$^{-/-}$ mice to lethal infection by this pathogen (25). In contrast, *Wdfy4*$^{-/-}$ mice are resistant to *T. gondii* infection, similar to *Wdfy4*$^{+/-}$ mice (Fig. 4C). These results indicate that cross-presentation is not required for innate protection against *T. gondii,* and that *Wdfy4*$^{-/-}$ cDC1 are not globally impaired in function.

We also evaluated $CD8^+$ T cell responses of *Wdfy4*$^{-/-}$ mice to cowpox virus infection, a model in which effective $CD8^+$ T cell priming is thought to be mediated primarily by *Batf3*-dependent cells through cross-presentation (73). *Batf3*$^{-/-}$ mice that lack cDC1 (10–13) have a defect in priming antigen-specific $CD8^+$ T cells to several viruses (10–13), but these

studies only indirectly show that this is due to a lack of cross-presentation, since a loss of alternative functions of cDC1 could conceivably be the cause. However, we now show that *Wdfy4*$^{-/-}$ mice, that retain cDC1 cells which cannot cross-present, also have a severely impaired antigen-specific CD8^{+} T cell responses to cowpox virus (Fig. 4D and E, fig. S14A to D). This defect in cross-presentation is not restricted to cowpox virus, since *Wdfy4*$^{-/-}$ mice also show a defect in priming CD8^{+} T cells to infection by West Nile virus (fig. S14E). However, *Wdfy4*$^{-/-}$ mice show normal priming of CD4^{+} T cells to West Nile, indicating that WDFY4 functions for *in vivo* cross-presentation to CD8^{+} T cells, but not for priming of CD4^{+} T cells (fig. S14F).

Studies with *Batf3*$^{-/-}$ mice suggested that cDC1 were required for tumor rejection (10). To examine the role of cross-presentation directly, we evaluated growth of the highly immunogenic 1969 regressor fibrosarcoma (15) in WT, *Wdfy4*$^{+/-}$, *Wdfy4*$^{-/-}$ and *Batf3*$^{-/-}$ mice (Fig. 4F). Tumors were readily rejected by WT mice, but not by *Batf3*$^{-/-}$ mice (Fig. 4F) as expected (15). However, tumors were also rejected by heterozygous *Wdfy4*$^{+/-}$ mice, but grew uncontrolled in *Wdfy4*$^{-/-}$ mice similar to *Batf3*$^{-/-}$ mice (Fig. 4F and S15A). These results with germline-deficient *Wdfy4*$^{-/-}$ mice indicate an *in vivo* requirement for WDFY4 in tumor rejection, but do not pinpoint its function to cDC1. To test whether the *in vivo* defect in *Wdfy4*$^{-/-}$ mice is cDC1-intrinsic, we generated mixed bone-marrow (BM) chimeras using mixtures of either WT: *Batf3*$^{-/-}$ or *Wdfy4*$^{-/-}$: *Batf3*$^{-/-}$ BM (Fig. 4G). WT: *Batf3*$^{-/-}$ chimeras rejected tumors normally, but *Wdfy4*$^{-/-}$: *Batf3*$^{-/-}$ chimeras, in which cDC1 develop only from the *Wdfy4*$^{-/-}$ BM, failed to control tumor growth (Fig. 4G). These results indicate that the defect in tumor rejection results from loss of Wdfy4 expression in cDC1. Notably, in *Wdfy4*$^{-/-}$ mice, cDC1 do infiltrate into tumors as they expand (Fig. 4H, fig. S15B), yet they induce less recruitment of CD8^{+} T cells to tumors, similar to the lack of CD8^{+} T cells in tumors in *Batf3* $^{-/-}$ mice (Fig. 4I).

WDFY4 is one of nine mammalian BEACH-domain containing proteins (BDCP) that typically also contain a PH-like domain and WD repeats (46). BDCP function as protein scaffolds that regulate intracellular vesicle fission and fusion events, and several are associated with human diseases (46). For example, mutations in *Lyst* cause the Chediak-Higashi syndrome, a primary immunodeficiency disorder characterized by defective neutrophil phagolysosome formation and cytotoxic T cell degranulation (63,64). Mutations in *Lrba* result in immune dysregulation in regulatory T cells due to improper trafficking of CTLA4 from endosomes to lysosomes by the clathrin adaptor AP-1 (65,66). WDFY3, the closest WDFY4 homolog, regulates recruitment of polyubiquitinated protein aggregates to autophagosomes by interactions with p62, Atg5, Atg12, Atg16L, LC3 and TRAF6 (67–70). Although cross-presentation of cell-associated antigens does not involve autophagy (71), WDFY4 conceivably may regulate vesicular trafficking pathways, a concept supported by its localization to submembrane endosomes and its interaction with endocytic and cytoskeletal machinery. These WDFY4-dependent trafficking pathways may be required for translocation of dead-cell antigen ligated by the cDC1-specific receptor CLEC9A (72) to specific compartments to promote cross-presentation (73). Further investigation of the mechanisms of WDFY4 may elucidate novel components of the cross-presentation pathway and thus offer therapeutic targets for human disease.

Supplementary Material

Refer to Web version on PubMed Central for supplementary material.

Acknowledgements:

We thank the Alvin J. Siteman Cancer Center at Washington University School of Medicine for use of the Center for Biomedical Informatics and Multiplex Gene Analysis Genechip Core Facility. We would like to thank E. Tonc for blinded microscopy analysis. We gratefully thank D. Oakley and J. Fitzpatrick for assistance with confocal microscopy which was performed at Washington University Center for Cellular Imaging (WUCCI). supported by Washington University School of Medicine, The Children's Discovery Institute of Washington University and St. Louis Children's Hospital (CDI-CORE-2015–505), the Foundation for Barnes-Jewish Hospital (3770) and the National Institute for Diabetes and Digestive and Kidney Diseases (P30 DK020579). We thank R. Tomaino and the Taplin mass spectrometry core at Harvard University for performing mass spectrometry experiments.

Funding: This work was supported by NIH grant T32 AI007163–40 (D.J.T.); NCI grants T32 CA 009621 (J.T.D.), 5R01 CA 190700 (R.D.S.), P30 CA 091842 (W.E.G.), 5R01 CA 193318 (N.M.); NIAID grant U19-Al109948 (W.Y.); NIH grant F30DK108498 (V.D.); NSF grant DGE-1143954 (P.B.); NIH grant U19-Al109725 (H.W.V.); Howard Hughes Medical Institute (K.M.M.). WDFY4-deficient mice used in this study were generated by the JAX KOMP program (U42OD011185).

Reference List

1. Blum JS, Wearsch PA, Cresswell P, Pathways of antigen processing Annu.Rev Immunol 31, 443–473 (2013). [PubMed: 23298205]
2. Murphy TL, Grajales-Reyes GE, Wu X, Tussiwand R, Briseno CG, Iwata A, Kretzer NM, Durai V, Murphy KM, Transcriptional Control of Dendritic Cell Development Annu.Rev Immunol 34, 93–119 (2016). [PubMed: 26735697]
3. Durai V, Murphy KM, Functions of Murine Dendritic Cells Immunity 45, 719–736 (2016). [PubMed: 27760337]
4. Guilliams M, Ginhoux F, Jakubzick C, Naik SH, Onai N, Schraml BU, Segura E, Tussiwand R, Yona S, Dendritic cells, monocytes and macrophages: a unified nomenclature based on ontogeny Nat.Rev.Immunol. 14, 571–578 (2014). [PubMed: 25033907]
5. Crozat K, Tamoutounour S, Vu Manh TP, Fossum E, Luche H, Ardouin L, Guilliams M, Azukizawa H, Bogen B, Malissen B, Henri S, Dalod M, Cutting edge: expression of XCR1 defines mouse lymphoid-tissue resident and migratory dendritic cells of the CD8alpha+ type J.Immunol. 187, 4411–4415 (2011). [PubMed: 21948982]
6. Bevan MJ, Cross-priming for a secondary cytotoxic response to minor H antigens with H-2 congenic cells which do not cross-react in the cytotoxic assay J Exp.Med. 143, 1283–1288 (1976). [PubMed: 1083422]
7. Joffre OP, Segura E, Savina A, Amigorena S, Cross-presentation by dendritic cells Nat.Rev.Immunol. 12, 557–569 (2012). [PubMed: 22790179]
8. den Haan JM, Lehar SM, Bevan MJ, CD8(+) but not CD8(−) dendritic cells cross-prime cytotoxic T cells in vivo J Exp.Med. 192, 1685–1696 (2000). [PubMed: 11120766]
9. Dudziak D, Kamphorst AO, Heidkamp GF, Buchholz VR, Trumpfheller C, Yamazaki S, Cheong C, Liu K, Lee HW, Park CG, Steinman RM, Nussenzweig MC, Differential antigen processing by dendritic cell subsets in vivo Science 315, 107–111 (2007). [PubMed: 17204652]
10. Hildner K, Edelson BT, Purtha WE, Diamond M, Matsushita H, Kohyama M, Calderon B, Schraml BU, Unanue ER, Diamond MS, Schreiber RD, Murphy TL, Murphy KM, Batf3 deficiency reveals a critical role for CD8alpha+ dendritic cells in cytotoxic T cell immunity Science 322, 1097–1100 (2008). [PubMed: 19008445]
11. Torti N, Walton SM, Murphy KM, Oxenius A, Batf3 transcription factor-dependent DC subsets in murine CMV infection: differential impact on T-cell priming and memory inflation EurJ.Immunol. 41, 2612–2618 (2011).

12. Nopora K, Bernhard CA, Ried C, Castello AA, Murphy KM, Marconi P, Koszinowski U, Brocker T, MHC class I cross-presentation by dendritic cells counteracts viral immune evasion Front Immunol. 3, 348 (2012). [PubMed: 23189079]
13. Gainey MD, Rivenbark JG, Cho H, Yang L, Yokoyama WM, Viral MHC class I inhibition evades CD8+ T-cell effector responses in vivo but not CD8+ T-cell priming Proc.Natl.Acad.Sci.U.S A (2012).
14. Fuertes MB, Kacha AK, Kline J, Woo SR, Kranz DM, Murphy KM, Gajewski TF, Host type I IFN signals are required for antitumor CD8+ T cell responses through CD8{alpha}+ dendritic cells J.Exp.Med. 208, 2005–2016 (2011). [PubMed: 21930765]
15. Diamond MS, Kinder M, Matsushita H, Mashayekhi M, Dunn GP, Archambault JM, Lee H, Arthur CD, White JM, Kalinke U, Murphy KM, Schreiber RD, Type I interferon is selectively required by dendritic cells for immune rejection of tumors J.Exp.Med. 208, 1989–2003 (2011). [PubMed: 21930769]
16. Toubai T, Sun Y, Luker G, Liu J, Luker KE, Tawara I, Evers R, Liu C, Mathewson N, Malter C, Nieves E, Choi S, Murphy KM, Reddy P, Host-derived CD8+ dendritic cells are required for induction of optimal graft-versus-tumor responses after experimental allogeneic bone marrow transplantation Blood 121, 4231–4241 (2013). [PubMed: 23520337]
17. Yu X, Guo C, Yi H, Qian J, Fisher PB, Subjeck JR, Wang XY, A multifunctional chimeric chaperone serves as a novel immune modulator inducing therapeutic antitumor immunity Cancer Res. 73, 2093–2103 (2013). [PubMed: 23333935]
18. Ali OA, Verbeke C, Johnson C, Sands RW, Lewin SA, White D, Doherty E, Dranoff G, Mooney DJ, Identification of immune factors regulating antitumor immunity using polymeric vaccines with multiple adjuvants Cancer Res. 74, 1670–1681 (2014). [PubMed: 24480625]
19. Zhang Y, Chen G, Liu Z, Tian S, Zhang J, Carey CD, Murphy KM, Storkus WJ, Falo LD Jr., You Z, Genetic vaccines to potentiate the effective CD103+ dendritic cell-mediated cross-priming of antitumor immunity J Immunol 194, 5937–5947 (2015). [PubMed: 25972487]
20. Tzeng A, Kauke MJ, Zhu EF, Moynihan KD, Opel CF, Yang NJ, Mehta N, Kelly RL, Szeto GL, Overwijk WW, Irvine DJ, Wittrup KD, Temporally Programmed CD8alpha(+) DC Activation Enhances Combination Cancer Immunotherapy Cell Rep. 17, 2503–2511 (2016). [PubMed: 27926855]
21. Sanchez-Paulete AR, Cueto FJ, Martinez-Lopez M, Labiano S, Morales- Kastresana A, Rodriguez-Ruiz ME, Jure-Kunkel M, Azpilikueta A, Aznar MA, Quetglas JI, Sancho D, Melero I, Cancer Immunotherapy with Immunomodulatory Anti- CD137 and Anti-PD-1 Monoclonal Antibodies Requires BATF3-Dependent Dendritic Cells Cancer Discov. 6, 71–79 (2016). [PubMed: 26493961]
22. Moynihan KD, Opel CF, Szeto GL, Tzeng A, Zhu EF, Engreitz JM, Williams RT, Rakhra K, Zhang MH, Rothschilds AM, Kumari S, Kelly RL, Kwan BH, Abraham W, Hu K, Mehta NK, Kauke MJ, Suh H, Cochran JR, Lauffenburger DA, Wittrup KD, Irvine DJ, Eradication of large established tumors in mice by combination immunotherapy that engages innate and adaptive immune responses Nat Med 22, 1402–1410 (2016). [PubMed: 27775706]
23. Kwan BH, Zhu EF, Tzeng A, Sugito HR, Eltahir AA, Ma B, Delaney MK, Murphy PA, Kauke MJ, Angelini A, Momin N, Mehta NK, Maragh AM, Hynes RO, Dranoff G, Cochran JR, Wittrup KD, Integrin-targeted cancer immunotherapy elicits protective adaptive immune responses J Exp Med 214, 1679–1690 (2017). [PubMed: 28473400]
24. Spranger S, Dai D, Horton B, Gajewski TF, Tumor-Residing Batf3 Dendritic Cells Are Required for Effector T Cell Trafficking and Adoptive T Cell Therapy Cancer Cell 31, 711–723 (2017). [PubMed: 28486109]
25. Mashayekhi M, Sandau MM, Dunay IR, Frickel EM, Khan A, Goldszmid RS, Sher A, Ploegh HL, Murphy TL, Sibley LD, Murphy KM, CD8a+ Dendritic Cells Are the Critical Source of Interleukin-12 that Controls Acute Infection by Toxoplasma gondii Tachyzoites Immunity 35, 249–259 (2011). [PubMed: 21867928]
26. Theisen D, Murphy K, The role of cDC1s in vivo: CD8 T cell priming through cross-presentation F1000Res. 6, 98 (2017). [PubMed: 28184299]
27. Sallusto F, Lanzavecchia A, Efficient presentation of soluble antigen by cultured human dendritic cells is maintained by granulocyte/macrophage colony-stimulating factor plus interleukin 4 and

downregulated by tumor necrosis factor alpha J Exp.Med. 179, 1109–1118 (1994). [PubMed: 8145033]

28. Caux C, Dezutter-Dambuyant C, Schmitt D, Banchereau J, GM-CSF and TNF-alpha cooperate in the generation of dendritic Langerhans cells Nature 360, 258–261 (1992). [PubMed: 1279441]
29. Inaba K, Inaba M, Romani N, Aya H, Deguchi M, Ikehara S, Muramatsu S, Steinman RM, Generation of large numbers of dendritic cells from mouse bone marrow cultures supplemented with granulocyte/macrophage colony-stimulating factor J ExpMed. 176, 1693–1702 (1992).
30. Helft J, Bottcher J, Chakravarty P, Zelenay S, Huotari J, Schraml BU, Goubau D, Sousa Reis E GM-CSF Mouse Bone Marrow Cultures Comprise a Heterogeneous Population of CD11c(+)MHCII(+) Macrophages and Dendritic Cells Immunity 42, 1197–1211 (2015). [PubMed: 26084029]
31. Briseno CG, Haldar M, Kretzer NM, Wu X, Theisen DJ, KC W, Durai V, Grajales-Reyes GE, Iwata A, Bagadia P, Murphy TL, Murphy KM, Distinct Transcriptional Programs Control Cross-Priming in Classical and Monocyte-Derived Dendritic Cells Cell Rep. 15, 2462–2474 (2016). [PubMed: 27264183]
32. Kretzer NM, Theisen DJ, Tussiwand R, Briseno CG, Grajales-Reyes GE, Wu X, Durai V, Albring J, Bagadia P, Murphy TL, Murphy KM, RAB43 facilitates cross-presentation of cell-associated antigens by CD8alpha+ dendritic cells J Exp.Med 213, 2871–2883 (2016). [PubMed: 27899443]
33. Kovacsovics-Bankowski M, Rock KL, A phagosome-to-cytosol pathway for exogenous antigens presented on MHC class I molecules Science 267, 243–246 (1995). [PubMed: 7809629]
34. Moron VG, Rueda P, Sedlik C, Leclerc C, In vivo, dendritic cells can cross-present virus-like particles using an endosome-to-cytosol pathway J Immunol 171, 2242–2250 (2003). [PubMed: 12928368]
35. Cruz FM, Colbert JD, Merino E, Kriegsman BA, Rock KL, The Biology and Underlying Mechanisms of Cross-Presentation of Exogenous Antigens on MHC-I Molecules Annu.Rev Immunol 35, 149–176 (2017). [PubMed: 28125356]
36. Pfeifer JD, Wick MJ, Roberts RL, Findlay K, Normark SJ, Harding CV, Phagocytic processing of bacterial antigens for class I MHC presentation to T cells Nature 361, 359–362 (1993). [PubMed: 7678924]
37. Shen L, Sigal LJ, Boes M, Rock KL, Important role of cathepsin S in generating peptides for TAP-independent MHC class I crosspresentation in vivo Immunity 21, 155–165 (2004). [PubMed: 15308097]
38. Cebrian I, Visentin G, Blanchard N, Jouve M, Bobard A, Moita C, Enninga J, Moita LF, Amigorena S, Savina A, Sec22b regulates phagosomal maturation and antigen crosspresentation by dendritic cells Cell 147, 1355–1368 (2011). [PubMed: 22153078]
39. Alloatti A, Rookhuizen DC, Joannas L, Carpier JM, Iborra S, Magalhaes JG, Yatim N, Kozik P, Sancho D, Albert ML, Amigorena S, Critical role for Sec22b-dependent antigen cross-presentation in antitumor immunity J Exp.Med 214, 2231–2241 (2017). [PubMed: 28663435]
40. Wu SJ, Niknafs YS, Kim SH, Oravecz-Wilson K, Zajac C, Toubai T, Sun Y, Prasad J, Peltier D, Fujiwara H, Hedig I, Mathewson ND, Khoriaty R, Ginsburg D, Reddy P, A Critical Analysis of the Role of SNARE Protein SEC22B in Antigen Cross-Presentation Cell Rep. 19, 2645–2656 (2017). [PubMed: 28658614]
41. Porgador A, Yewdell JW, Deng Y, Bennink JR, Germain RN, Localization, quantitation, and in situ detection of specific peptide-MHC class I complexes using a monoclonal antibody Immunity 6, 715–726 (1997). [PubMed: 9208844]
42. Harding CV, Unanue ER, Quantitation of antigen-presenting cell MHC class II/peptide complexes necessary for T-cell stimulation Nature 346, 574–576 (1990). [PubMed: 2115981]
43. Christinck ER, Luscher MA, Barber BH, Williams DB, Peptide binding to class I MHC on living cells and quantitation of complexes required for CTL lysis Nature 352, 67–70 (1991). [PubMed: 2062379]
44. Cong L, Ran FA, Cox D, Lin S, Barretto R, Habib N, Hsu PD, Wu X, Jiang W, Marraffini LA, Zhang F, Multiplex genome engineering using CRISPR/Cas systems Science 339, 819–823 (2013). [PubMed: 23287718]

45. Platt RJ, Chen S, Zhou Y, Yim MJ, Swiech L, Kempton HR, Dahlman JE, Parnas O, Eisenhaure TM, Jovanovic M, Graham DB, Jhunjhunwala S, Heidenreich M, Xavier RJ, Langer R, Anderson DG, Hacohen N, Regev A, Feng G, Sharp PA, Zhang F, CRISPR-Cas9 knockin mice for genome editing and cancer modeling Cell 159, 440–455 (2014). [PubMed: 25263330]

46. Cullinane AR, Schaffer AA, Huizing M, The BEACH is hot: a LYST of emerging roles for BEACH-domain containing proteins in human disease Traffic 14, 749–766 (2013). [PubMed: 23521701]

47. The UniProt Consortium, UniProt: the universal protein knowledgebase Nucleic Acids Res. 45, D158–D169 (2017). [PubMed: 27899622]

48. Schnorrer P, Behrens GM, Wilson NS, Pooley JL, Smith CM, El Sukkari D, Davey G, Kupresanin F, Li M, Maraskovsky E, Belz GT, Carbone FR, Shortman K, Heath WR, Villadangos JA, The dominant role of CD8+ dendritic cells in cross-presentation is not dictated by antigen capture Proc.Natl.Acad.Sci U.S.A 103, 10729–10734 (2006). [PubMed: 16807294]

49. Segura E, Albiston AL, Wicks IP, Chai SY, Villadangos JA, Different cross-presentation pathways in steady-state and inflammatory dendritic cells *Proc*.Natl.Acad.Sci.U.S A 106, 20377–20381 (2009).

50. McKay V, Moore EE. Immortalized Dendritic Cells. US Patent 5,648,219. 7–15-1997.

51. Bindea G, Mlecnik B, Hackl H, Charoentong P, Tosolini M, Kirilovsky A, Fridman WH, Pages F, Trajanoski Z, Galon J, ClueGO: a Cytoscape plug-in to decipher functionally grouped gene ontology and pathway annotation networks Bioinformatics 25, 1091–1093 (2009). [PubMed: 19237447]

52. Kaksonen M, Roux A, Mechanisms of clathrin-mediated endocytosis Nat Rev Mol Cell Biol 19, 313–326 (2018). [PubMed: 29410531]

53. Hedman AC, Smith JM, Sacks DB, The biology of IQGAP proteins: beyond the cytoskeleton EMBO Rep. 16, 427–446 (2015). [PubMed: 25722290]

54. Thomas DG, Robinson DN, The fifth sense: Mechanosensory regulation of alpha-actinin-4 and its relevance for cancer metastasis Semin CellDev.Biol 71, 68–74 (2017).

55. Jefferies KC, Cipriano DJ, Forgac M, Function, structure and regulation of the vacuolar (H+)-ATPases Arch.Biochem Biophys. 476, 33–42 (2008). [PubMed: 18406336]

56. Zheng H, Li Z, Cutting edge: cross-presentation of cell-associated antigens to MHC class I molecule is regulated by a major transcription factor for heat shock proteins J Immunol 173, 5929–5933 (2004). [PubMed: 15528326]

57. Ichiyanagi T, Imai T, Kajiwara C, Mizukami S, Nakai A, Nakayama T, Udono H, Essential role of endogenous heat shock protein 90 of dendritic cells in antigen cross-presentation J Immunol 185, 2693–2700 (2010). [PubMed: 20668218]

58. Imai T, Kato Y, Kajiwara C, Mizukami S, Ishige I, Ichiyanagi T, Hikida M, Wang JY, Udono H, Heat shock protein 90 (HSP90) contributes to cytosolic translocation of extracellular antigen for cross-presentation by dendritic cells Proc.Natl Acad.Sci.U S A 108, 16363–16368 (2011). [PubMed: 21930907]

59. Kato Y, Kajiwara C, Ishige I, Mizukami S, Yamazaki C, Eikawa S, Kakimi K, Udono H, HSP70 and HSP90 Differentially Regulate Translocation of Extracellular Antigen to the Cytosol for Cross-Presentation Autoimmune.Dis 2012, 745962 (2012).

60. Mellacheruvu D, Wright Z, Couzens AL, Lambert JP, St Denis NA, Li T, Miteva YV, Hauri S, Sardiu ME, Low TY, Halim VA, Bagshaw RD, Hubner NC, Al Hakim A, Bouchard A, Faubert D, Fermin D, Dunham WH, Goudreault M, Lin ZY, Badillo BG, Pawson T, Durocher D, Coulombe B, Aebersold R, Superti-Furga G, Colinge J, Heck AJ, Choi H, Gstaiger M, Mohammed S, Cristea IM, Bennett KL, Washburn MP, Raught B, Ewing RM, Gingras AC, Nesvizhskii AI, The CRAPome: a contaminant repository for affinity purification-mass spectrometry data Nat Methods 10, 730–736 (2013). [PubMed: 23921808]

61. Junttila MR, Saarinen S, Schmidt T, Kast J, Westermarck J, Single-step Strep-tag purification for the isolation and identification of protein complexes from mammalian cells Proteomics 5, 1199–1203 (2005). [PubMed: 15761952]

62. Osorio F, Tavernier SJ, Hoffmann E, Saeys Y, Martens L, Vetters J, Delrue I, De Rycke R, Parthoens E, Pouliot P, Iwawaki T, Janssens S, Lambrecht BN, The unfolded-protein-response

sensor IRE-lalpha regulates the function of CD8alpha+ dendritic cells Nat Immunol 15, 248–257 (2014). [PubMed: 24441789]

63. Perou CM, Moore KJ, Nagle DL, Misumi DJ, Woolf EA, McGrail SH, Holmgren L, Brody TH, Dussault BJ Jr., Monroe CA, Duyk GM, Pryor RJ, Li L, Justice MJ, Kaplan J, Identification of the murine beige gene by YAC complementation and positional cloning Nat Genet. 13, 303–308 (1996). [PubMed: 8673129]
64. Nagle DL, Karim MA, Woolf EA, Holmgren L, Bork P, Misumi DJ, McGrail SH, Dussault BJ Jr., Perou CM, Boissy RE, Duyk GM, Spritz RA, Moore KJ, Identification and mutation analysis of the complete gene for Chediak-Higashi syndrome Nat Genet. 14, 307–311 (1996). [PubMed: 8896560]
65. Lo B, Zhang K, Lu W, Zheng L, Zhang Q, Kanellopoulou C, Zhang Y, Liu Z, Fritz JM, Marsh R, Husami A, Kissell D, Nortman S, Chaturvedi V, Haines H, Young LR, Mo J, Filipovich AH, Bleesing JJ, Mustillo P, Stephens M, Rueda CM, Chougnet CA, Hoebe K, McElwee J, Hughes JD, Karakoc-Aydiner E, Matthews HF, Price S, Su HC, Rao VK, Lenardo MJ, Jordan MB, AUTOIMMUNE DISEASE. Patients with LRBA deficiency show CTLA4 loss and immune dysregulation responsive to abatacept therapy Science 349, 436–440 (2015). [PubMed: 26206937]
66. Lo B, Fritz JM, Su HC, Uzel G, Jordan MB, Lenardo MJ, CHAI and LATAIE: new genetic diseases of CTLA-4 checkpoint insufficiency Blood 128, 1037–1042 (2016). [PubMed: 27418640]
67. Simonsen A, Birkeland HC, Gillooly DJ, Mizushima N, Kuma A, Yoshimori T, Slagsvold T, Brech A, Stenmark H, Alfy, a novel FYVE-domain-containing protein associated with protein granules and autophagic membranes J Cell Sci. 117, 4239–4251 (2004). [PubMed: 15292400]
68. Clausen TH, Lamark T, Isakson P, Finley K, Larsen KB, Brech A, Overvatn A, Stenmark H, Bjorkoy G, Simonsen A, Johansen T, p62/SQSTM1 and ALFY interact to facilitate the formation of p62 bodies/ALIS and their degradation by autophagy Autophagy. 6, 330–344 (2010). [PubMed: 20168092]
69. Filimonenko M, Isakson P, Finley KD, Anderson M, Jeong H, Melia TJ, Bartlett BJ, Myers KM, Birkeland HC, Lamark T, Krainc D, Brech A, Stenmark H, Simonsen A, Yamamoto A, The selective macroautophagic degradation of aggregated proteins requires the PI3P-binding protein Alfy Mol Cell 38, 265–279 (2010). [PubMed: 20417604]
70. Isakson P, Lystad AH, Breen K, Koster G, Stenmark H, Simonsen A, TRAF6 mediates ubiquitination of KIF23/MKLP1 and is required for midbody ring degradation by selective autophagy Autophagy. 9, 1955–1964 (2013). [PubMed: 24128730]
71. Mintern JD, Macri C, Chin WJ, Panozza SE, Segura E, Patterson NL, Zeller P, Bourges D, Bedoui S, McMillan PJ, Idris A, Nowell CJ, Brown A, Radford KJ, Johnston AP, Villadangos JA, Differential use of autophagy by primary dendritic cells specialized in cross-presentation Autophagy. 11, 906–917 (2015). [PubMed: 25950899]
72. Sancho D, Joffre OP, Keller AM, Rogers NC, Martinez D, Hernanz-Falcon P, Rosewell I, Sousa Reis E, Identification of a dendritic cell receptor that couples sensing of necrosis to immunity Nature 458, 899–903 (2009). [PubMed: 19219027]
73. Zelenay S, Keller AM, Whitney PG, Schraml BU, Deddouche S, Rogers NC, Schulz O, Sancho D, Reis E Sousa, The dendritic cell receptor DNGR-1 controls endocytic handling of necrotic cell antigens to favor cross-priming of CTLs in virus-infected mice J.Clin.Invest 122, 1615–1627 (2012). [PubMed: 22505458]
74. Lybarger L, Wang X, Harris MR, Virgin HW, Hansen TH, Virus subversion of the MHC class I peptide-loading complex Immunity 18, 121–130 (2003). [PubMed: 12530981]
75. Sedy JR, Gavrieli M, Potter KG, Hurchla MA, Lindsley RC, Hildner K, Scheu S, Pfeffer K, Ware CF, Murphy TL, Murphy KM, B and T lymphocyte attenuator regulates T cell activation through interaction with herpesvirus entry mediator Nat.Immunol. 6, 90–98 (2005). [PubMed: 15568026]
76. Ran FA, Hsu PD, Wright J, Agarwala V, Scott DA, Zhang F, Genome engineering using the CRISPR-Cas9 system Nat Protoc. 8, 2281–2308 (2013). [PubMed: 24157548]
77. Sanjana NE, Shalem O, Zhang F, Improved vectors and genome-wide libraries for CRISPR screening Nat Methods 11, 783–784 (2014). [PubMed: 25075903]
78. Tussiwand R, Lee WL, Murphy TL, Mashayekhi M, Wumesh KC, Albring JC, Satpathy AT, Rotondo JA, Edelson BT, Kretzer NM, Wu X, Weiss LA, Glasmacher E, Li P, Liao W, Behnke M,

Lam SS, Aurthur CT, Leonard WJ, Singh H, Stallings CL, Sibley LD, Schreiber RD, Murphy KM, Compensatory dendritic cell development mediated by BATF-IRF interactions Nature 490, 502–507 (2012). [PubMed: 22992524]

79. Subauste C, Animal models for Toxoplasma gondii infection *Curr.Protoc.Immunol.***Chapter 19**, Unit-23 (2012).
80. Shankaran V, Ikeda H, Bruce AT, White JM, Swanson PE, Old LJ, Schreiber RD, IFNgamma and lymphocytes prevent primary tumour development and shape tumour immunogenicity Nature 410, 1107–1111 (2001). [PubMed: 11323675]
81. Lauron EJ, Yang L, Elliott JI, Gainey MD, Fremont DH, Yokoyama WM, Cross-priming induces immunodomination in the presence of viral MHC class I inhibition PLoS Pathog 14, e1006883 (2018).
82. Grajales-Reyes GE, Iwata A, Albring J, Wu X, Tussiwand R, KC W, Kretzer NM, Briseno CG, Durai V, Bagadia P, Haldar M, Schonheit J, Rosenbauer F, Murphy TL, Murphy KM, Batf3 maintains autoactivation of Irf8 for commitment of a CD8alpha(+) conventional DC clonogenic progenitor Nat Immunol 16, 708–717 (2015). [PubMed: 26054719]
83. Ardouin L, Luche H, Chelbi R, Carpentier S, Shawket A, Montanana SF, Santa MC, Grenot P, Alexandre Y, Gregoire C, Fries A, Vu Manh TP, Tamoutounour S, Crozat K, Tomasello E, Jorquera A, Fossum E, Bogen B, Azukizawa H, Bajenoff M, Henri S, Dalod M, Malissen B, Broad and Largely Concordant Molecular Changes Characterize Tolerogenic and Immunogenic Dendritic Cell Maturation in Thymus and Periphery Immunity 45, 305–318 (2016). [PubMed: 27533013]
84. Heng TS, Painter MW, Immunological Genome Project Consortium, The Immunological Genome Project: networks of gene expression in immune cells Nat Immunol 9, 1091–1094 (2008). [PubMed: 18800157]
85. Hsu PD, Scott DA, Weinstein JA, Ran FA, Konermann S, Agarwala V, Li Y, Fine EJ, Wu X, Shalem O, Cradick TJ, Marraffini LA, Bao G, Zhang F, DNA targeting specificity of RNA-guided Cas9 nucleases Nat Biotechnol. 31, 827–832 (2013). [PubMed: 23873081]

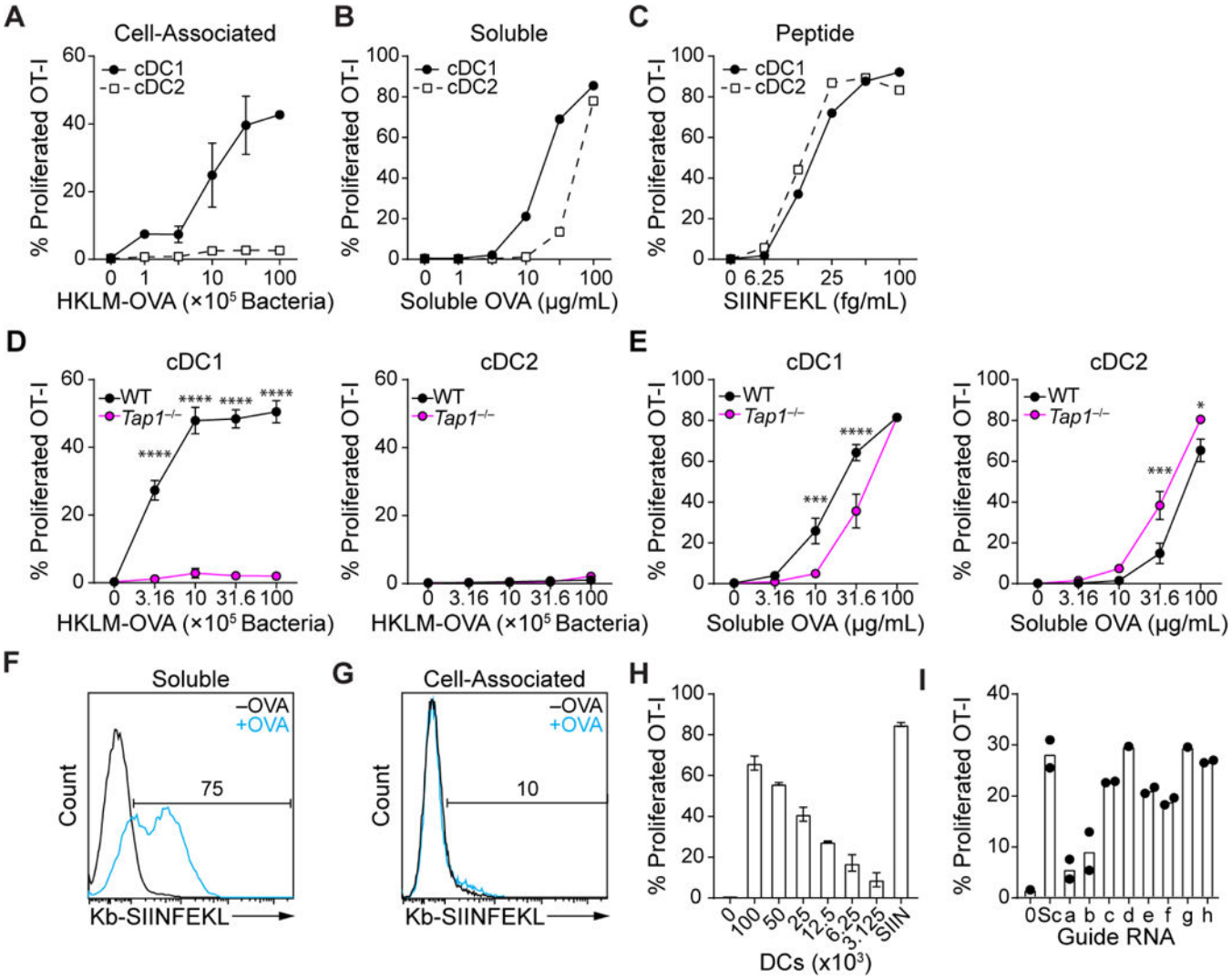

Fig. 1. Establishment of a CRISPR/Cas9 screen for cross-presentation of cell-associated antigens.

(A-C) Increasing concentrations of HKLM-OVA (A), soluble ovalbumin (B) or SIINFEKL peptide were cultured with sort-purified cDCland cDC2 for three days with CFSE-labeled OT-I T cells and assayed for proliferation ($CFSE^{-}CD44^{+}$). **(D, E)** WT or *Tap1*$^{-/-}$ sort-purified cDCl and cDC2 were cultured for three days with varying concentrations of HKLM-OVA (D) or soluble OVA (E) and CFSE-labeled OT-I T cells and assayed for proliferation ($CFSE^{-}CD44^{+}$). **(F-G)** Sorted cDCl were cultured with 100 μg/mL soluble ovalbumin (F) or 10^6 splenocytes osmotically loaded with OVA (G), cultured for 48 hours and stained with 25-D1.16 and analyzed by flow cytometry. **(H)** CFSE-labeled OT-I cells were cultured with the indicated number of whole Flt3L-generated DCs and 10^7 HKLM-OVA or 25 fg/mL SIINFEKL peptide (SIIN) and proliferation measured as in (A). **(I)** c-Kit^{hi} bone marrow progenitors from Cas9 transgenic mice were infected with retroviruses expressing various sgRNAs (Supplementary Table 2), cultured with Flt3L for seven days, and infected cDCs tested for cross-presentation to CFSE-labeled OT-I T cells as in (H), Sc=Scramble. Activated T cells gated as $CFSE^{-}CD44^{+}$. For all figures data indicate mean

±SEM. For all figures, statistical analysis was performed using 2-way ANOVA with Tukey's multiple comparisons test. * $P<0.05$; *** $P<0.001$; **** $P<0.0001$

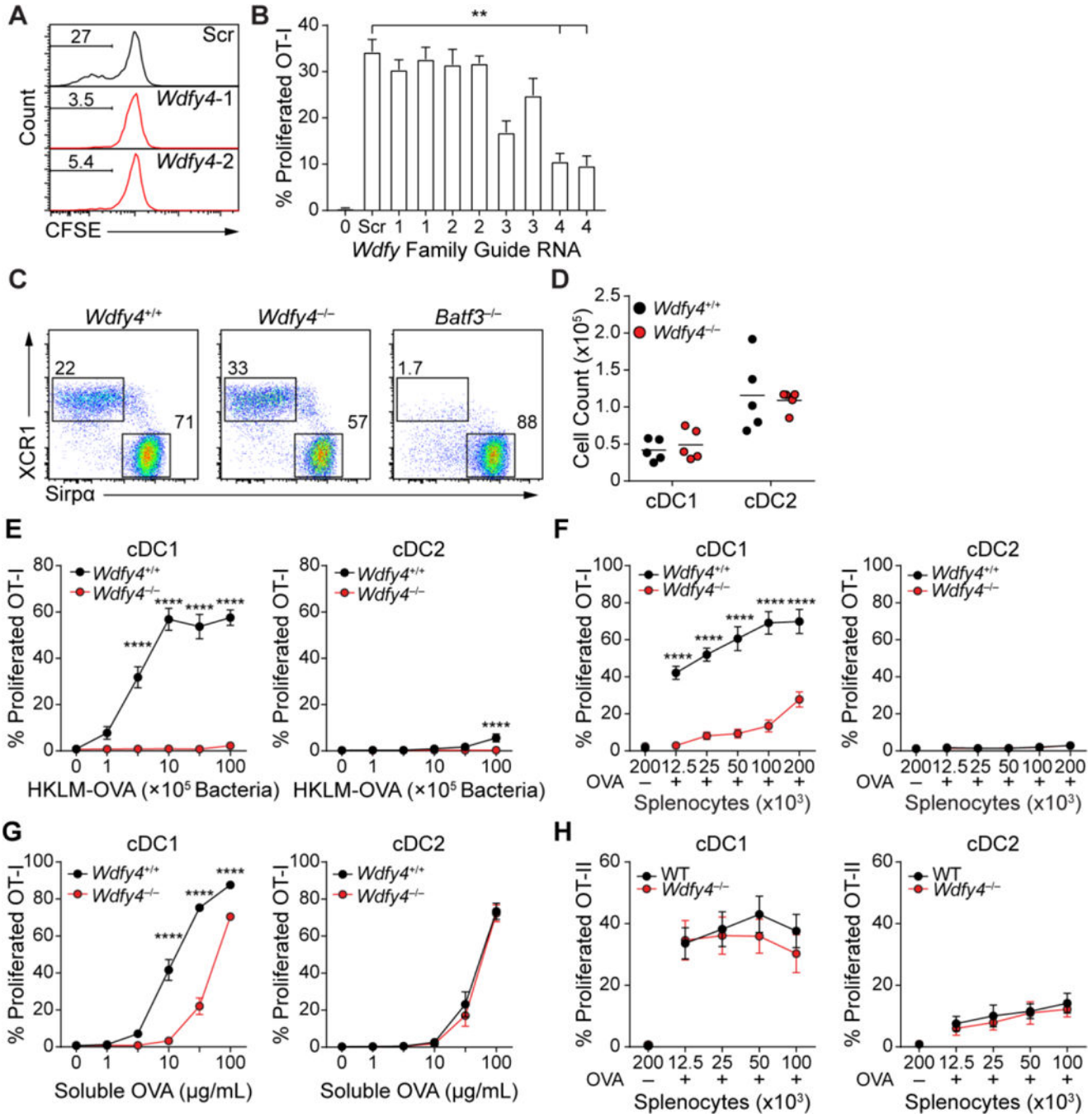

Fig. 2. *Wdfy4* is selectively required for cross-presentation of cell-associated antigens by cDC1.

(A) Cross-presentation was measured for Cas9-transgenic cDCl expressing two sgRNA (1 and 2; middle and bottom) for *Wdfy4* or a scramble control (top) that were generated as described in (Fig. 1I). T cell proliferation shown by percentages of $CFSE^{-}$ OT-I cells. **(B)** Cross-presentation by cDCl expressing sgRNAs for *Wdfy1, Wdfy2, Wdfy3* and *Wdfy4* was measured as described in (Fig. 1I). Scr=Scramble. Activated T cells gated as $CFSE^{-}CD44^{+}$. Data indicate mean ± SEM of 3 independent experiments **(C)** cDC1 and cDC2 development was assessed by flow cytometry in WT, *Wdfy4*$^{-/-}$ and *Batf3*$^{-/-}$ mice, plots were pre-gated as

B220^{-}CD11c^{+}MHCII^{+} and then gated as cDC1 (XCR1^{+}Sirpα^{-}) or cDC2 (XCR1^{-}Sirpα^{+}). **(D)** absolute cell numbers of cDC1 and cDC2 in WT and *Wdfy4*$^{-/-}$ mice. Each dot indicates one mouse, bar indicates mean. **(E)** FACS sorted cDC1 and cDC2 from spleens of WT and *Wdfy4*$^{-/-}$ mice were assayed for presentation to OT-I (CFSE^{-}CD44^{+}) in response to the indicated concentrations of HKLM-OVA. **(F)** FACS sorted cDC1 and cDC2 from spleens of bone marrow chimeric mice with WT or *Wdfy4*$^{-/-}$ bone marrow were assayed for presentation to OT-I (CFSE^{-}CD44^{+}) in response to indicated concentrations of OVA-loaded irradiated splenocytes from MHCI TKO mice. A negative control of splenocytes osmotically pulsed in the absence of OVA, OVA-, was included **(G)** FACS sorted cDC1 and cDC2 from spleens of WT and *Wdfy4*$^{-/-}$ mice were assayed for presentation to OT-I (CFSE^{-}CD44^{+}) in response to indicated concentrations of soluble OVA. **(H)** FACS sorted cDC1 and cDC2 from spleens of WT and *Wdfy4*$^{-/-}$ mice were assayed for presentation to OT-II (CFSE^{-}CD44^{+}) in response to indicated concentrations of OVA-loaded irradiated splenocytes from MHCII KO mice. A negative control of splenocytes osmotically pulsed in the absence of OVA, OVA-, was included. For all figures, data indicate mean ±SEM for three independent experiments, *P<0.05; **P<0.01; ****P<0.0001 using 2-way ANOVA with Tukey's multiple comparisons test.

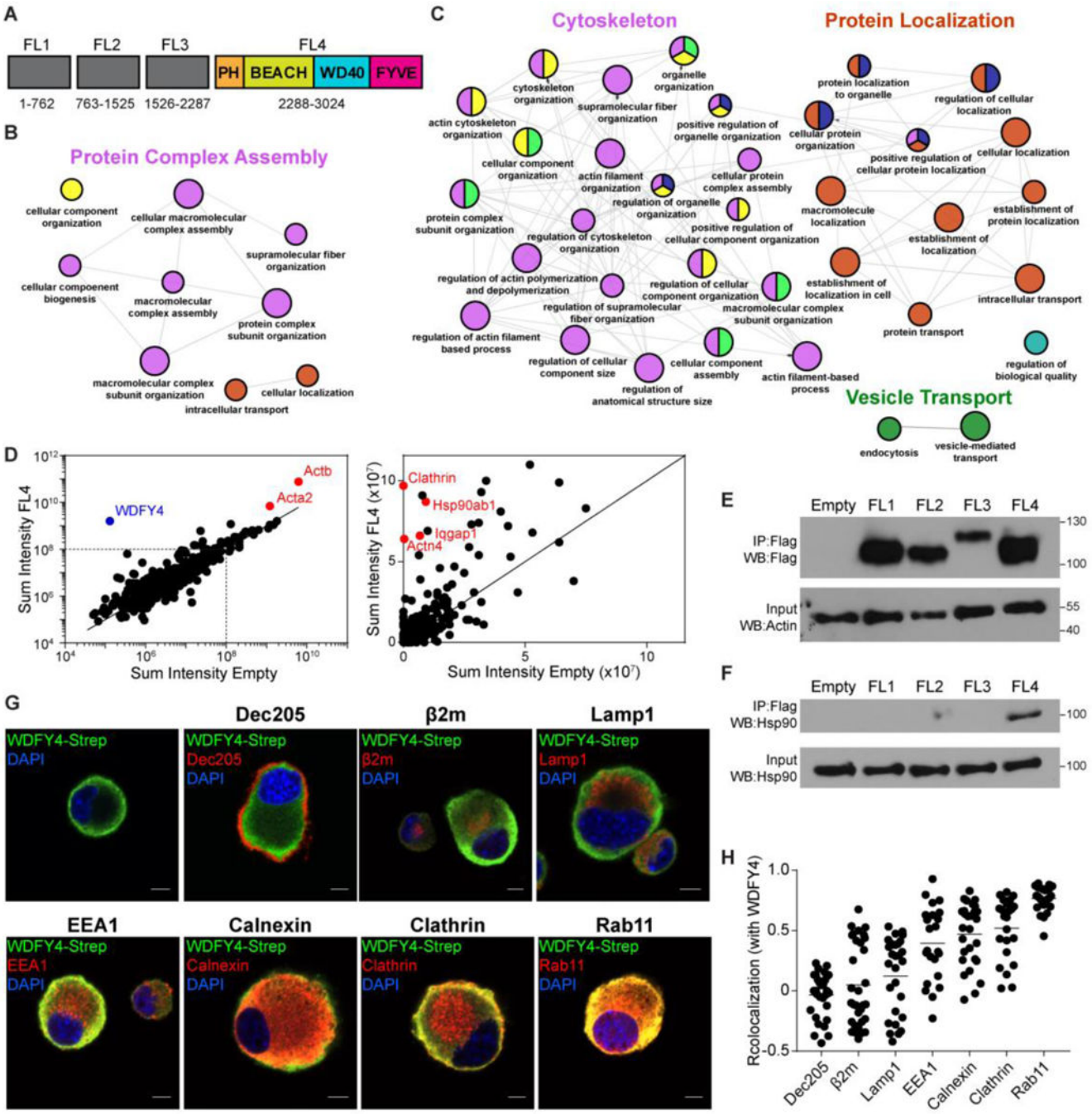

Fig. 3. WDFY4 acts near the plasma membrane and associates with proteins involved in localization and vesicular transport.

(A) Diagram of truncated fragments of WDFY4 protein, showing predicted domains within FL4 fragment. Numbers indicate amino-acid locations of fragments. **(B)** ClueGO visualization of gene ontology terms enriched after immunoprecipitation of fragments from (A) in the mouse DC line JAWSII, expressing either FL1 or FL2 fragments. Small circles $P<.001$, large circles $P<.0001$. Colors indicate Gene Ontology (GO) term groups. **(C)** ClueGO visualization of gene ontology terms enriched after immunoprecipitation of

fragments from (A) in the mouse DC line JAWSII expressing either FL3 or FL4 fragments. Small circles $P<3\times10^{-5}$, large circles $P<3\times10^{-6}$. Colors indicate GO term groups. **(D)** Scatterplot of representative data for sum intensity of proteins found after mass spectrometry between FL4 expressing and empty-vector expressing JAWSII cells. **(E)** Western blot of Flag immunoprecipitates from HEK293 cells transfected with empty-vector or Flag-tagged WDFY4 fragments 1 to 4 (top), and input control for β-actin (bottom) **(F)** Western blot for endogenous Hsp90 in Flag immunoprecipitates from HEK293 transfected with empty-vector or Flag-tagged WDFY4 fragments 1 to 4 (top) and input control for endogenous Hsp90 (bottom) **(G)** Confocal microscopy of JAWSII cells overexpressing full length Twin-Strep-tagged WDFY4, stained for anti-Strep (green), various cellular markers (red), and DAPI (blue). Scale bars indicate 5μm. **(H)** Quantification of co-localization between WDFY4 and intracellular markers from images in (G), each dot represents one cell, bar indicates the mean.

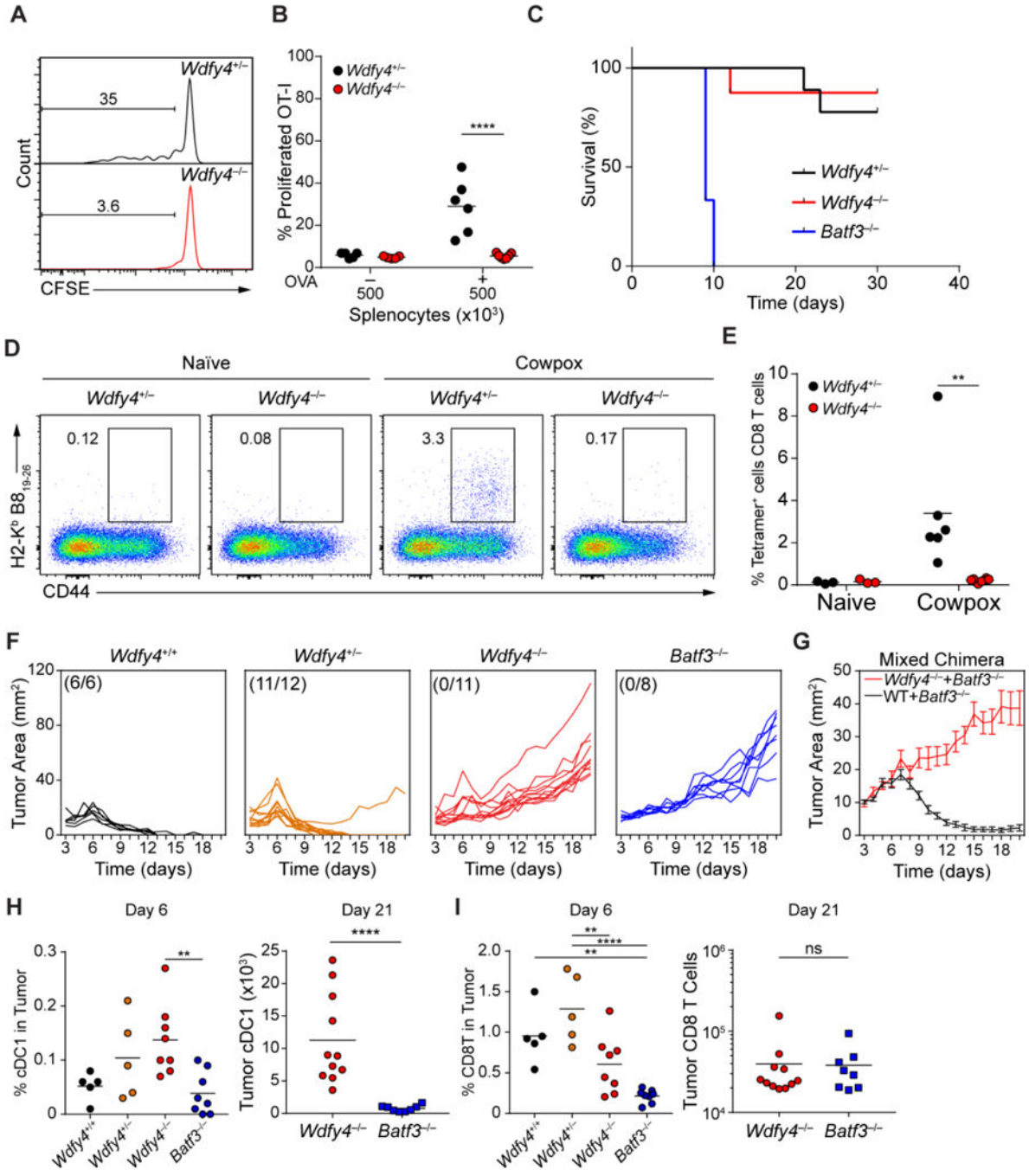

Fig. 4. *Wdfy4*$^{-/-}$ mice are unable to cross-present *in vivo*

(A-B) Representative flow cytometry analysis of *in vivo* cross-presentation to 500K irradiated splenocytes loaded with OVA injected i.v. into mice of the indicated genotypes one day after injection of 500K CFSE-labeled OT-I cells. Mice were harvested three days after antigen injection, quantified in (B). Data pre-gated on OT-I cells and shown as percentage of CFSE^{-} cells (A) or CFSE^{-}CD44^{+} cells (B). Data are pooled from three independent experiments; each point represents one mouse. **(C)** Survival of mice of the indicated genotypes to injection of 200 Pru.luc *T. gondii* tachyzoites over 30 days.

WDFY4$^{+/-}$ n=9, *WDFY4*$^{-/-}$ n=8, *Batf3*$^{-/-}$ n=3. **(D-E)** Representative flow cytometry plots of CD8 T cells (pre-gate CD4^{-}CD3^{+}CD8^{+}) in lungs of naïve or cowpox infected mice, quantified in (E). Each dot represents one mouse, bar indicates mean. **(F)** Mice of the indicated genotypes were injected with 1×10^{6} fibrosarcoma cells s.c. and tumors were measured daily starting at day three after injection. **(G)** Mixed bone marrow chimeras with bone marrow of indicated genotypes were injected into lethally irradiated CD45.1^{+} WT B6 mice. Eight weeks later, mice were injected with 1×10^{6} fibrosarcoma cells s.c. and tumors were measured daily starting at day three after injection. Data show mean ± SEM of 9 mice per group. **(H)** Quantification of cDC1 in tumors at either day 6 or day 21 after injection taken from mice of indicated genotypes. Gated as B220^{-}CD11c^{+}MHCII^{+}CD103^{+}CD11b^{-}. Each dot indicates one mouse, bar indicates mean. **(I)** Quantification of CD8 T cells in tumors at either day 6 or day 21 after injection taken from mice of indicated genotypes. Gated as CD45^{+}TCRβ^{+}CD8α^{+}CD4^{-}. Each dot indicates one mouse, bar indicates mean. For all figures, ** P<.01; **** P<0.0001 using 2-way ANOVA with Tukey's multiple comparisons test.